Holzforschung, Vol. 59, pp. 620–627, 2005 • Copyright © by Walter de Gruyter • Berlin • New York. DOI 10.1515/HF.2005.100

Structure-activity relationships of cadinane-type sesquiterpene derivatives against wood-decay fungi

Chi-Lin Wu[1], Shih-Chang Chien[2], Sheng-Yang Wang[3], Yueh-Hsiung Kuo[2] and Shang-Tzen Chang[1,*]

[1] School of Forestry and Resource Conservation, National Taiwan University, Taipei, Taiwan
[2] Department of Chemistry, National Taiwan University, Taipei, Taiwan
[3] Department of Forestry, National Chung-Hsing University, Taichung, Taiwan

*Corresponding author.
School of Forestry and Resource Conservation, National Taiwan University, No. 1, Section 4 Roosevelt Road, Taipei 106, Taiwan
Tel.: +886-2-33664626
Fax: +886-2-23654520
E-mail: peter@ntu.edu.tw

Abstract

Cadinane-type sesquiterpenes have a wide spectrum of biological activity, but their use as wood preservatives and the structure-activity relationships of their derivatives have not yet been reported. A total of 13 compounds were synthesized from T-cadinol, T-muurolol, and α-cadinol and their chemical structures were confirmed by IR, MS, and ^{1}H and ^{13}C NMR. The antifungal properties of 16 compounds against three wood-decay fungi were evaluated *in vitro*. α-Cadinol showed strong antifungal activity against *Lenzites betulina*, *Trametes versicolor*, and *Laetiporus sulphureus* (total mean IC_{50} 0.10 mM). Among the derivatives synthesized, 3β-ethoxy-T-muurolol (0.24 mM), 4ξ*H*-cadinan-10β-ol (0.25 mM), 4ξ*H*-muurolan-10β-ol (0.29 mM), and 4ξ*H*-cadinan-10α-ol (0.25 mM) showed good antifungal activity against all fungi tested. Correlation was observed between the antifungal activity of the compounds tested and log *P*. Furthermore, the presence of an unsaturated double bond and oxygen-containing functional groups in the compounds plays a key role in their antifungal activity. The stereo configuration of cadinane-type sesquiterpenes also influences their antifungal activity. Understanding how the structure of natural compounds relates to their antifungal function is important and may facilitate their application as novel wood preservatives.

Keywords: cadinane-type sesquiterpene; α-cadinol; 4ξ*H*-cadinan-10α-ol; 4ξ*H*-cadinan-10β-ol; 3β-ethoxy-T-muurolol; log *P*; 4ξ*H*-muurolan-10β-ol; structure-activity relationship; wood-decay fungi.

Introduction

Natural products have attracted increasing interest as ecologically safer alternatives to fungicides and insecticides and as sources of new medicines. Over the past few years, fungicide research has produced a diverse range of products with novel modes of action that are expected to have a significant impact on disease control in the next decade (McChesney 1993; Grayer and Harbone 1994; Oliva et al. 2003). Recently, great interest has been focused on natural products and wood extracts for resistance against wood-decay fungi. Understanding the capability of wood extracts to protect against fungi is one possible approach for developing new fungicides (Celimene et al. 1999; Schultz and Nicholas 2002). Furthermore, the discovery of an array of natural antifungal substances is of vital importance in overcoming the continuing development of microbial resistance in agriculture.

Biodegradation of wood by fungi is a serious problem for both wooden structures and forest management. Basidiomycete fungi of the genera *Trametes*, *Lenzites*, and *Laetiporus* are recognized worldwide as major wood-decay fungi. Failure to control them can result in serious economic losses to the wood industry and agriculture. Most lumber from the US is produced in the southeast, and over half of all southern yellow-pine dimension stock is chemically treated in some manner, principally with a preparation referred to as chromated copper arsenate. The environmental hazards associated with the use of both chromium and arsenic salts will likely adversely limit their future use. Therefore, the desire for safer phytochemicals with lower environmental and mammalian toxicity is a major concern (Schultz and Nicholas 2000; Wedge et al. 2000).

Sesquiterpenes possess a wide spectrum of biological activity through which they appear to play a role in plant defense mechanisms (Fraga 2001, 2003). Due to their bioactivity, some sesquiterpenes with the cadinane skeleton have been evaluated for antifungal or insecticidal activity. Cadinane-type sesquiterpenes constitute a fairly large family of more than 200 compounds mainly isolated from the woody parts of plants, and they are often associated with decay resistance.

In our previous studies (Chang et al. 1998, 1999, 2000a, 2001), we have demonstrated that the wood of Taiwania (*Taiwania cryptomerioides*), one of the most important plantation softwoods in Taiwan, is a species with excellent antifungal and antitermitic properties. In addition, it has been proven that cadinane skeletal sesquiterpenes, including T-cadinol, T-muurolol and α-cadinol, are the predominant compounds in the heartwood of Taiwania. Results obtained from antifungal assays demonstrated that α-cadinol exhibited the highest antifungal activity for both *Trametes versicolor* and *Laetiporus sulphureus*, followed by T-cadinol and T-muurolol. Further comparison of the molecular configuration of these cadinanes revealed that cadinane skeletal sesquiterpenes with an equatorial hydroxyl group at C-10 and

a *trans*-fused configuration at the ring junction, as in α-cadinol, exhibited the strongest antifungal activity (Chang et al. 2000a). Moreover, there have also been reports stating that cadinanes have a significant effect in durable tree species against fungi and termites (Kondo and Imamura 1986; Kinjo et al. 1988). On the other hand, Labbe et al. (1993) demonstrated that T-cadinol shows significant toxicity to *Artemia salina* (brine shrimp bioassay). He et al. (1997) reported that α-cadinol showed bioactivity against brine shrimp, yellow fever mosquito (*Aedes aegypti*) larvae, and human tumor cells (HT-29). Similarly, in previous studies we found that α-cadinol was moderately active against HT-29, and T-muurolol was modestly active against both the HT-29 and MCF-7 cell lines (Chang et al. 2000b). To the best of our knowledge, no antifungal activity of the cadinane derivatives has been reported, so this property appeared to be worthy of evaluation. The present study describes the antifungal characteristics of 16 natural and semi-synthetic cadinane-type sesquiterpenes in antifungal assays, and explains the structure-activity relationship of the cadinane moiety.

Materials and methods

Plant material

Samples from 27-year-old Taiwania were collected from the experimental forest of the National Taiwan University located in Nantou County in central Taiwan.

General instruments

High-performance liquid chromatography (HPLC) was carried out using a Hitachi model L-7150 pump equipped with a L7490 refractive index detector and a Hibar Lichrosorb Si 60 (25 × 1 cm i.d.) column. IR spectra were recorded on a Bio-Rad FTS-40 instrument. Mass spectra (MS) were obtained on a Finnigan MAT-95S mass spectrometer. ^{1}H and ^{13}C NMR spectra were recorded on a Bruker DMX500 spectrometer at 500 MHz.

NMR analyses

The samples were dissolved in $CDCl_3$, and tetramethylsilane (TMS) was used as an internal standard. The ^{1}H, ^{13}C, COSY, NOESY, HMQC, and HMBC NMR spectra were recorded using standard pulse sequences of the instrument. For ^{1}H NMR, the chemical shifts (δ) are reported in parts per million (ppm) relative to TMS. The δ values were referenced to $CDCl_3$ (7.27 ppm). First-order behavior was assumed in analysis of ^{1}H NMR spectra, and multiplicities are as indicated by one or more of the following: s, singlet; d, doublet; t, triplet; m, multiplet; and br, broad. Spin coupling constants (*J* values) are reported to the nearest 0.5 Hz. For ^{13}C NMR, the δ values were referenced to $CDCl_3$ (77.23 ppm).

Extraction and isolation of three cadinanes

Three natural compounds, T-cadinol (**1**), T-muurolol (**2**) and α-cadinol (**3**), were isolated and purified from the heartwood of Taiwania according to the method described in our previous study (Chang et al. 2000a).

Hydrogenation of cadinane derivatives

The synthesis is outlined in Scheme 1. T-Cadinol (116.8 mg), T-muurolol (105.7 mg), or α-cadinol (66.6 mg) and Pd/C (10%) in 5 ml of methanol were stirred for 16 h under hydrogen. The reaction mixture was filtered through Celite to yield three products, 4ξ*H*-cadinan-10β-ol (**14**) (73.6 mg), 4ξ*H*-muurolan-10β-ol (**15**) (76.1 mg) and 4ξ*H*-cadinan-10α-ol (**16**) (47.3 mg).

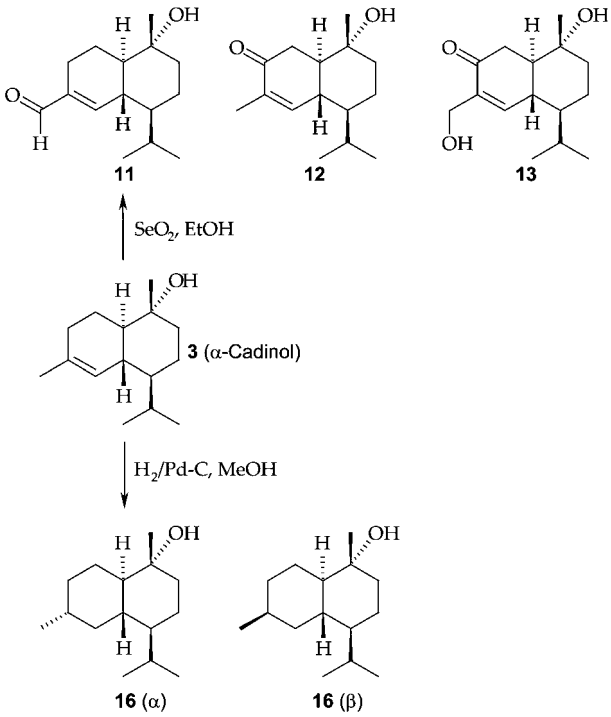

Scheme 1 Synthesis of four derivatives of α-cadinol.

Preparation and isolation of cadinane derivatives

The synthesis is outlined in Scheme 1. T-Cadinol (1.72 g), T-muurolol (1.58 g)nb, or α-cadinol (1.54 g) and SeO_2 (1.07 g) in 30 ml of 95% ethanol were refluxed for 6 h. The reaction mixture was filtrated through Celite, and the filtrate was chromatographed on a silica gel column by elution with gradients of *n*-hexane and EtOAc. 15-Oxo-T-cadinol (**4**) [retention time (RT) 11.9 min] and 3-oxo-T-cadinol (**5**) (RT 15.1 min) were isolated from the EA-3 fraction using a mobile phase of CH_2Cl_2/EtOAc/*n*-Hex (10:25:65) at a flow rate of 2.0 ml min^{-1}. 3-Oxo-15-hydroxy-T-cadinol (**6**) (RT 25.1 min) was isolated from EA-5, and then the mobile phase was changed to CH_2Cl_2/EtOAc/*n*-Hex (10:40:50). 15-Oxo-T-muurolol (**7**) (RT 13.0 min) and 3-oxo-T-muurolol (**8**) (RT 15.5 min) were obtained from EA-8 using a mobile phase of CH_2Cl_2/EtOAc/*n*-Hex (10:30:60). 3β-Hydroxy-T-muurolol (**9**) in the form of colorless crystals was separated from the EA-12 fraction during separation. 3β-Ethoxy-T-muurolol (**10**) (RT 11.7 min) (mobile phase CH_2Cl_2/EtOAc/*n*-Hex 10:30:60, flow rate 2.0 ml min^{-1}) was purified from the EA-7 fraction. 15-Oxo-α-cadinol (**11**) (RT 17.2 min) and 3-oxo-α-cadinol (**12**) (RT 23.5 min) were separated from the EA-10 fraction using a mobile phase of CH_2Cl_2/EtOAc/*n*-Hex (5:30:65). 3-Oxo-15-hydroxy-α-cadinol (**13**) was purified from the EA-14 fraction on the same HPLC system at 29.2 min using a mobile phase of CH_2Cl_2/EtOAc/*n*-Hex (10:40:50) at a flow rate of 2.0 ml min^{-1}. The chemical structures of the compounds isolated are shown in Figure 1.

15-Oxo-T-cadinol (**4**) Yellowish amorphous solid. EIMS m/z: 236 [M^+]. ^{13}C NMR ($CDCl_3$) data are listed in Table 1. ^{1}H NMR ($CDCl_3$) data are listed in Table 2.

3-Oxo-T-cadinol (**5**) Yellowish crystals, m.p. 97–98°C. EIMS m/z: 236 [M^+]. ^{1}H and ^{13}C NMR data coincided with those in the literature (Lin et al. 1974; Taber et al. 1996).

3-Oxo-15-hydroxy-T-cadinol (**6**) Yellowish amorphous solid. EIMS m/z: 252 [M^+]. ^{13}C NMR ($CDCl_3$) data are listed in Table 1. ^{1}H NMR ($CDCl_3$) data are listed in Table 2.

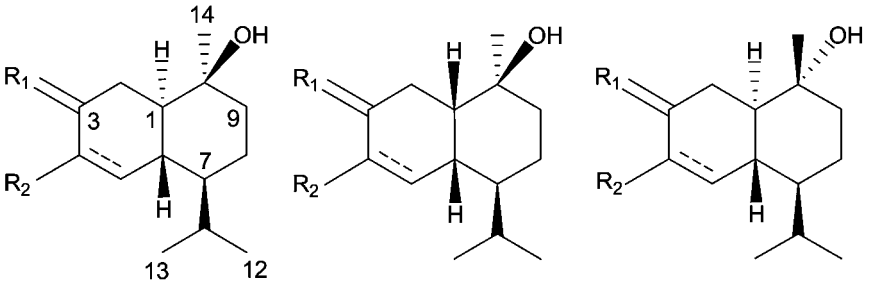

1 R_1=H_2, R_2=Me, Δ^4
4 R_1=H_2, R_2=CHO, Δ^4
5 R_1=O, R_2=Me, Δ^4
6 R_1=O, R_2=CH_2OH, Δ^4
14 R_1= H_2, R_2=Me (α+β)

2 R_1=H_2, R_2=Me, Δ^4
7 R_1=H_2, R_2=CHO, Δ^4
8 R_1=O, R_2=Me, Δ^4
9 R_1=β-OH, R_2=Me, Δ^4
10 R_1=α-OEt, R_2=Me, Δ^4
15 R_1= H_2, R_2=Me (α+β)

3 R_1=H_2, R_2=Me, Δ^4
11 R_1=H_2, R_2=CHO, Δ^4
12 R_1=O, R_2=Me, Δ^4
13 R_1=O, R_2= CH_2OH, Δ^4
16 R_1= H_2, R_2=Me (α+β)

Figure 1 Configurations of cadinane derivatives: T-cadinol (**1**), T-muurolol (**2**), α-cadinol (**3**), 15-oxo-T-cadinol (**4**), 3-oxo-T-cadinol (**5**), 3-oxo-15-hydroxy-T-cadinol (**6**), 15-oxo-T-muurolol (**7**), 3-oxo-T-muurolol (**8**), 3β-hydroxy-T-muurolol (**9**), 3β-ethoxy-T-muurolol (**10**), 15-oxo-α-cadinol (**11**), 3-oxo-α-cadinol (**12**), 3-oxo-15-hydroxy-α-cadinol (**13**), 4ξ*H*-cadinan-10β-ol (**14**), 4ξ*H*-muurolan-10β-ol (**15**), 4ξ*H*-cadinan-10α-ol (**16**).

15-Oxo-T-muurolol (**7**) Yellowish amorphous solid. EIMS m/z: 236 [M^+]. ^{13}C NMR ($CDCl_3$) data are listed in Table 1. ^{1}H NMR ($CDCl_3$) data are listed in Table 2.

3-Oxo-T-muurolol (**8**) Colorless crystals, m.p. 126–127°C. EIMS m/z: 236 [M^+]. ^{13}C NMR ($CDCl_3$) data are listed in Table 1. ^{1}H NMR ($CDCl_3$) data are listed in Table 2.

3β-Hydroxy-T-muurolol (**9**) Colorless crystals, m.p. 168–170°C. EIMS m/z: 238 [M^+]. ^{13}C NMR ($CDCl_3$) data are listed in Table 1. ^{1}H NMR ($CDCl_3$) data are listed in Table 2.

3β-Ethoxy-T-muurolol (**10**) Yellowish amorphous solid. EIMS m/z: 266 [M^+]. ^{13}C NMR ($CDCl_3$) data are listed in Table 1. ^{1}H NMR ($CDCl_3$) data are listed in Table 2.

15-Oxo-α-cadinol (**11**) Yellowish amorphous solid. EIMS m/z: 236 [M^+]. ^{1}H NMR data coincided with those in the literature (Kuo et al. 2002). ^{13}C NMR ($CDCl_3$) data are listed in Table 1.

3-Oxo-α-cadinol (**12**) Colorless crystals, m.p. 111–112°C. EIMS m/z: 236 [M^+]. ^{13}C NMR ($CDCl_3$) data are listed in Table 1. ^{1}H NMR ($CDCl_3$) data are listed in Table 2.

3-Oxo-15-hydroxy-α-cadinol (**13**) Yellowish amorphous solid. EIMS m/z: 252 [M^+]. ^{13}C NMR ($CDCl_3$) data are listed in Table 1. ^{1}H NMR ($CDCl_3$) data are listed in Table 2.

4ξ*H*-Cadinan-10β-ol (**14**)+4-epimer Colorless amorphous solid. EIMS m/z: 224 [M^+]. ^{1}H NMR ($CDCl_3$) data are listed in Table 2.

4ξ*H*-Muurolan-10β-ol (**15**)+4-epimer Colorless amorphous powder. EIMS m/z: 224 [M^+]. ^{1}H NMR ($CDCl_3$) data are listed in Table 2.

4ξ*H*-Cadinan-10α-ol (**16**)+4-epimer Colorless amorphous powder. EIMS m/z: 224 [M^+]. ^{1}H NMR ($CDCl_3$) data are listed in Table 2.

Chemical properties

The octanol/water partition coefficient (log *P*) of the compounds tested in this study was provided by the ChemDraw Ultra 9.0 software package (ChemOffice 2005, CambridgeSoft, Cambridge, MA, USA). IC_{50} values of compounds that were experimentally determined to be >200 μg ml^{-1} were assumed to be 1.0 mM to allow the inclusion of these compounds in analysis of the structure-activity relationships.

Antifungal assays

The fungi used were *Lenzites betulina* (BCRC 35296), *Trametes versicolor* (BCRC 35253), and *Laetiporus sulphureus* (BCRC 35305). *In vitro* antifungal assays were performed as in our previous study (Chang et al. 2000a). Assays were carried out in triplicate and the data were averaged. Different concentrations of the compounds (25, 50, 100, and 200 μg ml^{-1}) were added to sterilized potato dextrose agar (PDA). A commercial fungicide, didecyl dimethyl ammonium chloride (DDAC), was used as a positive control. The test plates were incubated at 26±2°C. When the mycelium of fungi reached the edges of the control plates, the antifungal index and median inhibitory concentrations (IC_{50}, mM) were calculated. The antifungal index was calculated as follows:

$$\text{Antifungal index (\%)} = (1 - D_a/D_b) \times 100$$

where D_a is the diameter of the growth zone in the experimental dish (cm) and D_b is the diameter of the growth zone in the control dish (cm).

Statistical analyses

All results obtained from three independent experiments are expressed as mean±SD. Significant differences ($P < 0.05$) were determined by the Scheffe test.

Results and discussion

Identification of cadinane-type sesquiterpene derivatives

Oxidation of T-cadinol (**1**) with SeO_2 yielded the three derivatives **4**, **5**, and **6**. Compound **4** was isolated as an amorphous substance and showed a molecular ion at m/z 236 for $C_{15}H_{24}O_2$. The IR spectrum of **4** showed bonds attributable to a conjugated aldehyde (2735, 1685, and 1642 cm^{-1}). The ^{1}H NMR spectrum showed signals for an isopropyl group at 0.83 and 0.94 ppm (each 3H, d, J=6.9 Hz, H-12, H-13), and 2.03 ppm (1H, m, H-11), a three-proton singlet at 1.16 ppm (s, H-14) for a methyl attached to a quaternary carbon bearing a hydroxyl group, a trisubstituted olefinic proton at 6.90 ppm (s, H-5), and a conjugated aldehyde signal at 9.39 ppm (s, H-15). The ^{1}H NMR spectrum was very close to that of the starting product **1**. Major differences were observed for signals corresponding to the conjugated aldehyde group and the H-5 signal was shifted downfield. The ^{13}C

Table 1 ^{13}C NMR spectral data for cadinane sesquiterpene derivatives (**4–13**).

Position	δ (ppm)									
	4	**5**	**6**	**7**	**8**	**9**	**10**	**11**	**12**	**13**
1	47.9	49.9	49.4	48.0	45.8	42.8	42.6	49.7	51.1	50.7
2	21.5	38.5	38.4	21.2	34.2	30.8	26.0	21.5	38.3	38.5
3	22.2	201.0	201.2	26.4	199.5	68.7	76.1	22.2	200.2	200.9
4	141.4	134.8	137.3	134.3	134.8	134.3	132.6	141.9	135.3	137.8
5	153.0	147.7	148.8	142.4	151.0	129.9	130.2	152.0	146.1	147.6
6	39.6	38.7	38.5	33.9	35.7	34.9	34.3	41.5	40.8	40.6
7	45.9	45.0	44.7	45.5	43.2	40.4	40.8	45.7	45.0	44.8
8	26.7	26.4	26.3	28.2	27.9	27.3	27.3	22.3	21.5	21.5
9	40.3	39.9	39.7	38.6	37.2	34.9	34.6	41.8	41.5	41.4
10	70.7	69.7	69.6	70.6	71.2	72.2	71.5	72.1	71.1	71.1
11	28.8	27.9	27.8	28.5	28.7	29.5	29.4	26.3	26.1	26.2
12	21.5	21.3	21.2	19.7	21.4	21.7	21.6	21.4	21.4	21.4
13	15.5	15.3	15.1	15.7	15.9	15.7	15.5	15.3	15.1	15.1
14	20.2	19.4	19.3	16.0	19.5	21.3	19.2	20.6	20.9	20.8
15	194.7	15.9	61.2	194.7	16.0	19.3	21.1	194.7	15.8	61.4
OCH_2CH_3							64.6			
OCH_2CH_3							15.8			

Data acquired at 500 MHz in $CDCl_3$.

NMR data (Table 1) exhibited 15 carbon signals for an aldehyde, three CH_3, four CH_2, two olefinic carbons, four CH, and one C. Furthermore, the ^1H NMR data (Table 2) of **4** was similar to that of 15-oxo-α-cadinol (Kuo et al. 2002), except for differences attributable to the β-hydroxy group in **4**. On the basis of the above evidence, compound **4** was determined to be 15-oxo-T-cadinol. By comparing the NMR data for compound **5** with that of reported data (Lin et al. 1974; Taber et al. 1996), the structure of **5** was determined as 3-oxo-T-cadinol. EIMS revealed compound **6** to be a sesquiterpene with molecular formula $C_{15}H_{24}O_3$. The ^{13}C NMR data (Table 1) for **6** showed 15 carbon signals for a carbonyl (201.2 ppm), a double bond (148.8 and 137.3 ppm), an oxygenated carbon (69.6 ppm), three methyl groups, four methylenes, and four methines. The ^1H NMR data (Table 2) for **6** were similar to those for **5**. The main differences observed were in the position of the H-5 (7.03 ppm, s) and H-15 (4.17 ppm, 2H, s) signals, which were both shifted downfield because of a hydroxymethyl group attached to an olefinic group. Thus, based on the above evidence, the structure of compound **6** was established as 3-oxo-15-hydroxy-T-cadinol.

Oxidation of T-muurolol (**2**) yielded four derivatives, **7**, **8**, **9**, and **10**. The ^1H NMR data for compound **7** were very close to those for 15-oxo-T-cadinol (**4**), except for differences attributable to the *cis*-fused ring in **7**. Comparing the ^1H and ^{13}C NMR data for compound **7** with those for **4**, the structure of **7** was determined as 15-oxo-T-muurolol. Moreover, by comparison of ^1H NMR data for compounds **8** and **9** with reported data (Lin et al. 1974), the structures of **8** and **9** were determined as 3-oxo-T-muurolol and 3β-hydroxy-T-muurolol, respectively. However, the ^{13}C NMR data for compounds **8** and **9** are reported for the first time. Compound **10** was isolated as a solid substance and showed a molecular ion at m/z 266 for $C_{17}H_{30}O_2$. The ^{13}C NMR data (Table 1) for **10** showed 15 carbon signals for a double bond (132.6, 130.2 ppm), two oxygenated carbons (C and CH, 71.5, 76.1 ppm), five CH_3, four CH_2, and four CH. Ethoxyl signals were at 3.38 and 3.58 ppm (each 1H, m), and 1.16 ppm (3H, t, $J=7.0$ Hz). A broad signal at 3.47 ppm (1H, br s, H-2, resonating at 75.8 ppm), which showed HMBC correlation with 64.5 ppm ($-OCH_2CH_3$) and NOESY correlation with signals at 3.38 and 3.58 ppm ($-OCH_2CH_3$), was assigned as geminal to an ethoxyl group. An isopropyl group (0.79 and 0.82 ppm, each 3H, d, $J=6.9$ Hz; 2.25 ppm, 1H, m), a singlet methyl signal (1.13 ppm) on a quaternary carbon bearing a hydroxyl group, and a trisubstituted olefinic proton (5.71 ppm, d, $J=5.0$ Hz) were also observed. The presence of a doublet coupling ($J=5.0$ Hz) with H-6 for the olefinic proton H-5 revealed the *cis*-fused ring in **10**. NOESY and HMBC analyses confirmed the carbon signal assignments and the stereochemical structure of this compound. There was no NOESY correlation between H-1 and H-3, while there was NOEY correlation between H-1 and the β-axial ethoxyl group. Therefore, the structure of compound **10** was determined to be 3β-ethoxy-T-muurolol.

Oxidation of α-cadinol (**3**) afforded the three derivatives **11**, **12**, and **13**. Compound **13** had IR, EIMS, and ^1H NMR spectra similar to **6**. Comparing the ^1H and ^{13}C NMR spectra of **13** with 3-oxo-15-hydroxy-T-cadinol (**6**), the structure of **13** was determined as 3-oxo-15-hydroxy-α-cadinol. Furthermore, by comparison of ^1H NMR data for the two derivatives **11** and **12** with reported data (Kuo et al. 2002; Lin et al. 1974), the structures of **11** and **12** were determined as 15-oxo-α-cadinol and 3-oxo-α-cadinol, respectively. The ^{13}C NMR data for **11** and **12** are reported here for the first time. The hydrogenation of T-cadinol, T-muurolol, and α-cadinol yielded three products (**14–16**) and their 4-epimers. Their structures were elucidated by ^1H NMR (Table 2). Furthermore, NMR data for eight derivatives (**4**, **6**, **7**, **10**, **13–16**) are reported for the first time.

Antifungal activity of cadinane-type sesquiterpene and its derivatives

The results of antifungal tests (Figure 2) indicate that compounds **1–4**, **10**, **14**, **15**, and **16** were most active against *L. sulphureus*, with antifungal indices higher than 50.6%; while compounds **5–9** and **11–13** were the least

Table 2 ^{1}H NMR spectral data for cadinane sesquiterpene derivatives (**1–16**).

Compound	δ (ppm)							
	H3α	H5	H12	H13	H14	H15	OCH_2CH_3	OCH_2CH_3
1		5.52 (s)	0.76 (d, J = 7.0 Hz)	0.88 (d, J = 7.0 Hz)	1.19 (s)	1.70 (s)		
2		5.53 (d, J = 6.3 Hz)	0.80 (d, J = 7.0 Hz)	0.86 (d, J = 7.0 Hz)	1.16 (s)	1.62 (s)		
3		5.46 (s)	0.74 (d, J = 7.0 Hz)	0.89 (d, J = 7.0 Hz)	1.08 (s)	1.64 (s)		
4		6.90 (s)	0.84 (d, J = 6.9 Hz)	0.94 (d, J = 6.9 Hz)	1.16 (s)	9.39 (s)		
5		6.78 (s)	0.73 (d, J = 6.9 Hz)	0.86 (d, J = 6.9 Hz)	1.07 (s)	1.65 (s)		
6		7.03 (s)	0.77 (d, J = 6.9 Hz)	0.90 (d, J = 6.9 Hz)	1.12 (s)	4.17 (s)		
7		6.87 (d, J = 5.0 Hz)	0.75 (d, J = 6.9 Hz)	0.82 (d, J = 6.9 Hz)	1.13 (s)	9.30 (s)		
8		6.90 (d, J = 5.0 Hz)	0.84 (d, J = 6.9 Hz)	0.86 (d, J = 6.9 Hz)	1.12 (s)	1.72 (s)		
9	3.93 (s)	5.74 (d, J = 5.0 Hz)	0.83 (d, J = 6.9 Hz)	0.86 (d, J = 6.9 Hz)	1.23 (s)	1.78 (s)		
10	3.47 (br s)	5.69 (d, J = 5.0 Hz)	0.79 (d, J = 6.9 Hz)	0.82 (d, J = 6.9 Hz)	1.13 (s)	1.70 (s)	3.35, 3.58 (m)	1.16 (t, J = 7.0 Hz)
11		6.80 (s)	0.78 (d, J = 6.9 Hz)	0.91 (d, J = 6.9 Hz)	1.07 (s)	9.36 (s)		
12		6.76 (s)	0.79 (d, J = 6.9 Hz)	0.94 (d, J = 6.9 Hz)	1.12 (s)	1.74 (s)		
13		6.97 (s)	0.78 (d, J = 6.9 Hz)	0.93 (d, J = 6.9 Hz)	1.11 (s)	4.20 (s)		
14			0.69 (d, J = 6.9 Hz)	0.84 (d, J = 6.9 Hz)	1.13 (s)	0.94 (s)		
15			0.72 (d, J = 6.9 Hz)	0.79 (d, J = 6.9 Hz)	1.10 (s)	0.87 (s)		
16			0.67 (d, J = 6.9 Hz)	0.85 (d, J = 6.9 Hz)	1.09 (s)	0.93 (s)		

active, with antifungal indices lower than 29.4%. Furthermore, compounds **1–3** and **14–16** completely inhibited the growth of *L. sulphureus* at a concentration of 100 μg ml^{-1}. Similarly, compounds **1**, **3**, **4**, **10**, **14**, and **16** were very active against *T. versicolor*, while compounds **6**, **8**, **12**, and **13** were the least active. Furthermore, compounds **1–3**, **7–12** and **14–16** were highly efficient against *L. betulina*, with antifungal indices higher than 60.6%, while compounds **5**, **6**, and **13** were modestly active.

By comparing the IC_{50} values for all fungi (Table 3), a difference between the tolerances against the tested compounds can be observed. *T. versicolor* showed greater tolerance, with IC_{50} values higher than those determined for *L. sulphureus* for nine of the 16 compounds tested. For the six oxidized derivatives (**7–13**), *L. sulphureus* showed greater tolerance, with IC_{50} values higher than those determined for *L. betulina*. This can be attributed to the fact that brown- and white-rot fungi decay woods via distinctly different mechanisms. *T. versicolor* produces extracellular laccase, which catalyzes oxidation and thus inactivates the added compounds. Brown-rot fungi such as *L. sulphureus* cause the degradation of cellulose and hemicellulose in the cell wall, leaving lignin essentially undigested or, in some cases, demethylated, oxidized, or slightly depolymerized. Degradation of cellulose and lignin is the consequence of hydroxyl radical attack, which is generated through the Fenton reaction. The initial stages of brown-rot fungal decay involve oxidative degradation (Green and Highley 1997; Highley and Dashek 1998).

Fitzgerald (2005) demonstrated that the total mean MIC for structure-function analysis gives a good indication of the overall antimicrobial effectiveness resulting from specific sensitivity or resistance exhibited by an individual organism to certain compounds. The total mean IC_{50} values of the cadinane-type sesquiterpene derivatives are shown in Table 3. For all of the compounds examined, the total mean IC_{50} values varied, but the antifungal order of the compounds remained unchanged.

Structure-activity relationship of cadinane-type sesquiterpenes

The results also demonstrate a potential relationship between the chemical structure and the experimentally determined antifungal activity of the cadinane-type sesquiterpene compounds tested. Using total mean IC_{50}, the antifungal activity order of hydrogenated derivatives was 4ξ*H*-cadinan-10β-ol (**14**) (0.25 mM) = 4ξ*H*-cadinan-10α-ol (**16**) (0.25 mM) > 4ξ*H*-muurolan-10β-ol (**15**) (0.29 mM). Comparison with the total mean IC_{50} values of the original compounds indicates that derivatives **14** and **15** have increased antifungal activity, while derivative **16** has slightly decreased antifungal activity compared to the parent compounds. These results suggest that the unsaturated double bond in the compounds has an influence on their antifungal properties. Further comparisons of the molecular configuration of these derivatives revealed a similar result for the cadinane skeletal sesquiterpenes (**1–3**). Accordingly, a *trans*-fused configuration at the ring junction exhibited the strongest antifungal activity. It was

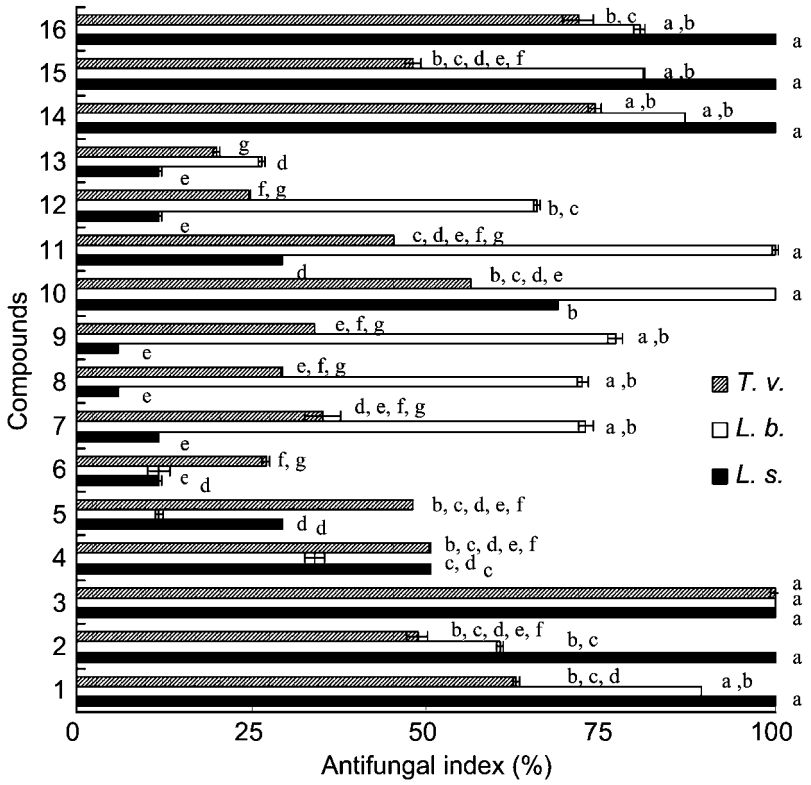

Figure 2 Antifungal activity of 16 compounds (100 μg ml^{-1}) against two white-rot fungi *L. betulina* and *T. versicolor* and the brown rot fungus *L. sulphureus*. Each experiment was performed three times and the data were averaged (n = 3). Numbers followed by different letters (a–g) are significantly different at the level of $P < 0.05$ according to the Scheffe test.

also noted that the stereo configuration of hydroxyl at C-10 was less important than the configuration at the ring junction.

Oxidized derivatives (**4**–**6** and **11**–**13**) with a *trans*-fused configuration at the ring junction with more than one oxygen-containing group (-OH, -CHO, -CO, -CH_2OH) in the ring exhibited lower antifungal activity. The position of the functional group in the ring also plays an important role in antifungal activity. Functional groups in the C-3 position of the ring decreased the antifungal activity of a compound compared to those with a methyl group. This was observed as a difference in the total mean IC_{50}, with 0.31 mM for T-cadinol (**1**) and 0.48 mM for 15-oxo-T-cadinol (**4**). In addition, the presence of a 3-oxo moiety in the ring strongly decreased the antifungal activity. For example, the IC_{50} values of 3-oxo-T-cadinol (**5**), 3-oxo-T-muurolol (**8**) and 3-oxo-α-cadinol (**12**) were higher than 0.85 mM, especially against *T. versicolor*.

On the other hand, oxidized derivatives (**7**–**10**) with an axial hydroxyl group at C-10 and a *cis*-fused configuration at the ring junction with more than one oxygen-containing group (-CO, -CHO, -OH, -OEt) in the ring

Table 3 IC_{50} values of cadinane sesquiterpene derivatives against wood decay fungi.

Compound	MW	IC_{50} (mM)			
		L. betulina	*T. versicolor*	*L. sulphureus*	Total mean
1	222	0.33	0.34	0.25	0.31
2	222	0.42	0.36	0.26	0.35
3	222	0.13	0.14	0.04	0.10
4	236	0.57	0.46	0.41	0.48
5	236	>0.85	0.71	0.66	>0.85
6	252	>0.79	>0.79	>0.79	>0.79
7	236	0.39	>0.85	>0.85	>0.85
8	236	0.25	>0.85	>0.85	>0.85
9	238	0.24	>0.84	>0.84	>0.84
10	266	0.15	0.31	0.26	0.24
11	236	0.20	0.49	0.72	0.47
12	236	0.31	>0.85	>0.85	>0.85
13	252	0.50	>0.79	>0.79	>0.79
14	224	0.30	0.30	0.16	0.25
15	224	0.33	0.38	0.17	0.29
16	224	0.31	0.29	0.16	0.25
DDAC	362	0.03	0.05	0.01	0.03

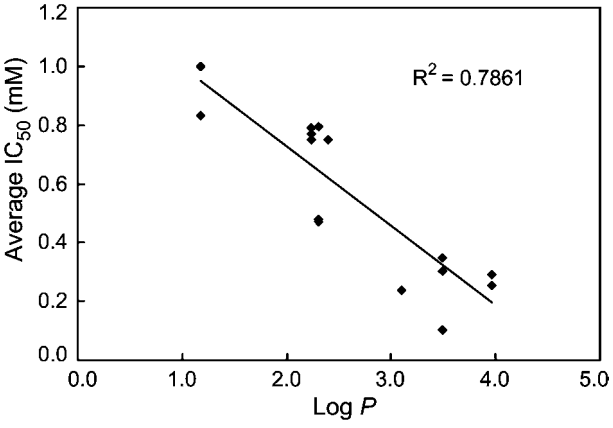

Figure 3 Relationship between the octanol/water partition coefficient (log *P*) and total mean IC_{50} of the cadinane sesquiterpene derivatives. (IC_{50} values of compounds that were experimentally determined to be greater than 200 μg ml^{-1} were assumed to be 1.0 mM to allow the inclusion of these compounds in analysis of the structure-activity relationships.)

exhibited greater inhibitory activity limited to *L. betulina*. Furthermore, functional groups in the C-3 position of the ring strongly increased the antifungal activity. Based on tests, the order of antifungal effectiveness of four derivatives against *L. betulina* was 3β-ethoxy-T-muurolol (**10**) (0.15 mM) > 3β-hydroxy-T-muurolol (**9**) (0.24 mM), 3-oxo-T-muurolol (**8**) (0.25 mM) > 15-oxo-T-muurolol (**7**) (0.39 mM). Comparisons with the IC_{50} values of the original compound (**2**) (0.42 mM) indicated that three oxidized derivatives (**7**–**10**) have significantly increased antifungal activity against *L. betulina*.

The relationships between log *P* and the antifungal activity of the compounds tested, taken as the total mean IC_{50} values, are presented in Figure 3. The most active compounds (**1**–**3**, **10**, **14**–**16**) against the test fungi are the most hydrophobic compounds in the data set, with calculated log *P* values ranging from 3.10 to 3.96, while the least active compounds (**6** and **13**) are the least hydrophobic (log *P* = 1.17). These data suggest that the hydrophobicity of compounds is an important factor for their antifungal activity. Knobloch et al. (1989) reported that the variation in fungicidal action of essential oil components depends on their hydrophilic and hydrophobic properties, which governs their capacity to penetrate the chitin cell walls of fungal hyphae. Voda et al. (2004) demonstrated that the log *P* value of oxygenated aromatic essential oil compounds could be used as a strong molecular descriptor for modeling of the experimentally determined MIC for *T. versicolor* and *C. puteana*. In addition, the antimicrobial activity of phenolic compounds correlates well with their intrinsic hydrophobicity and log *P* values (Ultee et al. 2002). Moreover, the geometry of the inhibitory compounds also plays a significant role in the binding of a substrate to an enzyme's active sites and thus affects their antifungal activity (Voda et al. 2003).

Conclusions

With regard to environmental protection, the search for environmentally friendly preservatives from highly durable tree species represents one approach for improving wood protection. We investigated the structure-activity relationships of 16 natural and semi-synthetic cadinane-type sesquiterpenes against wood-decay fungi. Among 16 compounds, α-cadinol exhibited the highest antifungal activity, followed by 3β-ethoxy-T-muurolol, 4ξ*H*-cadinan-10β-ol, and 4ξ*H*-cadinan-10α-ol. Clearly, the presence of the double bond and oxygen-containing functional groups in these compounds has an influence on their antifungal properties. In addition, the stereo configuration of cadinane-type sesquiterpenes also influences their activity. Furthermore, log *P* is a good indicator of antifungal activity for cadinane-type sesquiterpenes. Finally, T-cadinol, T-muurolol, and α-cadinol are the predominant components in Taiwania and are also widely present in the woody parts of numerous plants. Thus, understanding the influence of cadinane structures on durability could be helpful in designing and developing more effective wood preservatives.

Acknowledgements

The authors thank Ms Shou-Ling Huang (The Instrumentation Center of National Taiwan University) for the measurement of NMR spectra and Bioresources Collection and Research Center for providing the fungi.

References

Celimene, C.C., Micales, J.A., Ferge, L., Young, R.A. (1999) Efficacy of pinosylvins against white-rot and brown-rot fungi. Holzforschung 53:491–497.

Chang, S.T., Wu, C.L., Wang, S.Y., Su, Y.C., Kuo, Y.H. (1998) Studies on the antifungal compounds in the heartwood extractives of Taiwania (*Taiwania cryptomerioides* Hayata) (I): Isolation and identification of antifungal compounds in hexane soluble fraction (in Chinese with English abstract). For. Prod. Ind. 17:287–304.

Chang, S.T., Wang, S.Y., Wu, C.L., Su, Y.C., Kuo, Y.H. (1999) Antifungal compounds in the ethyl acetate soluble fraction of the extractives of Taiwania (*Taiwania cryptomerioides* Hayata) heartwood. Holzforschung 53:487–490.

Chang, S.T., Wang, S.Y., Wu, C.L., Chen, P.F., Kuo, Y.H. (2000a) Comparisons of the antifungal activities of cadinane skeletal sesquiterpenoids from Taiwania (*Taiwania cryptomerioides* Hayata) heartwood. Holzforschung 54:241–245.

Chang, S.T., Wang, D.S.Y., Wu, C.L., Shiah, S.G., Kuo, Y.H., Chang, C.J. (2000b) Cytotoxicity of extractives from *Taiwania cryptomerioides* heartwood. Phytochemistry 55:227–232.

Chang, S.T., Cheng, S.S., Wang, S.Y. (2001) Antitermitic activity of essential oils and components from Taiwania (*Taiwania cryptomerioides*). J. Chem. Ecol. 27:717–724.

Fitzgerald, D.J. (2005) Structure-function analysis of the vanillin molecule and its antifungal properties. J. Agric. Food Chem. 53:1769–1775.

Fraga, B.M. (2001) Natural sesquiterpenoids. Nat. Prod. Rep. 18:650–673.

Fraga, B.M. (2003) Natural sesquiterpenoids. Nat. Prod. Rep. 20:392–413.

Grayer, R., Harbone, J. (1994) A survey of antifungal compounds from higher plants. Phytochemistry 37:19–42.

Green, F. III, Highley, T.L. (1997) Mechanism of brown-rot decay: paradigm or paradox. Int. Biodeterior. Biodegrad. 39: 113–124.

Highley, T.L., Dashek, W.V. (1998) Biotechnology in the study of brown- and white-rot decay. In: Forest Products Biotechnology. Eds. Bruce, A., Palfreyman, J.W. Taylor & Francis, London. pp. 15–36.

He, K., Zeng, L., Shi, G., Zhao, G.X., Kozlowski, J.F., McLaughlin, J.L. (1997) Bioactive compounds from *Taiwania cryptomerioides* Hayata. J. Nat. Prod. 60:38–40.

Kinjo, K., Doufuku, Y., Yaga, S. (1988) Termiticidal substances from the wood of *Chamaecyparis obtusa*. Mokuzai Gakkaishi 34:451–455.

Knobloch, K., Pauli, A., Iberl, B., Weigand, H., Weis, N. (1989) Antibacterial and antifungal properties of essential oil components. J. Ess. Oil Res. 1:119–128.

Kondo, R., Imamura, H. (1986) Antifungal compounds in heartwood extractives of hinoki (*Chamaecyparis obtusa* Endl.). Mokuzai Gakkaishi 32:213–217.

Kuo, Y.H., Chen, C.H., Chien, S.C., Lin, Y.L. (2002) Five new cadinane-type sesquiterpenes from the heartwood of *Chamaecyparis obtusa* var. *formosana*. J. Nat. Prod. 65:25–28.

Labbe, C., Castillo, M., Connolly, J.D. (1993) Mono and sesquiterpenoids from *Satureja gilliesii*. Phytochemistry 34: 441–444.

Lin, Y.T., Chen, Y.S., Kuo, Y.H., Lin, K.C. (1974) NMR study of some sesquiterpene alcohols and their oxidation products. J. Chin. Chem. Soc. 21:31–35.

McChesney, J.D. (1993) Biological and chemical diversity and the search for new pharmaceuticals and other bioactive natural products. In: Human Medicinal Agents from Plants. Eds. Kinghorn, A.D., Balandrin, M.F. American Chemical Society, Washington, DC. pp. 38–47.

Oliva, A., Meepagala, K.M., Wedge, D.E., Harries, D., Hale, A.L., Aliotta, G., Duke, S.O. (2003) Natural fungicides from *Ruta graveolens* L. leaves, including a new quinolone alkaloid. J. Agric. Food Chem. 51:890–896.

Schultz, T.P., Nicholas, D.D. (2000) Naturally durable heartwood: evidence for a proposed dual defensive function of the extractives. Phytochemistry 54:47–52.

Schultz, T.P., Nicholas, D.D. (2002) Development of environmentally benign wood preservatives based on the combination of organic biocides with antioxidants and metal chelators. Phytochemistry 61:555–560.

Taber, D.F., Christos, T.E., Hodge, C.N. (1996) Cyclohexenone annelation by alkylidene C–H insertion: Synthesis of oxo-T-cadinol. J. Org. Chem. 61:2081–2084.

Ultee, A., Bennik, M.H.J. Moezelaar, R. (2002) The phenolic hydroxyl group of carvacrol is essential for action against the food-borne pathogen *Bacillus cereus*. Appl. Environ. Microbiol. 68:1561–1568.

Wedge, D.E., Galindo, J.C.G., Macias, F.A. (2000) Fungicidal activity of natural and synthetic sesquiterpene lactone analogs. Phytochemistry 53:747–757.

Voda, K., Boh, B., Vrtačnik, M., Pohleven, F. (2003) Effect of the antifungal activity of oxygenated aromatic essential oil compounds on the white-rot *Trametes versicolor* and the brown-rot *Coniophora puteana*. Int. Biodeterior. Biodegrad. 51: 51–59.

Voda, K., Boh, B., Vrtačnik, M. (2004) A quantitative structure-antifungal activity relationship study of oxygenated aromatic essential oil compounds using data structuring and PLS regression analysis. J. Mol. Model. 10:76–84.

Received May 18, 2005. Accepted July 8, 2005.